

Buckling Analysis of Piezolaminated Plates Using Higher Order Shear Deformation Theory

Rajan L. Wankhade*, Kamal M. Bajoria

Department of Civil Engineering, Indian Institute of Technology, Bombay, Mumbai, India

Abstract Buckling analysis of piezolaminated plate subjected to combined action of electro-mechanical loading is considered for the present work. Higher order shear deformation theory based finite element method is used to perform the analysis. An isoparametric eight noded element is employed in the finite element formulation. Studies are conducted for different ply orientation and plate aspect ratios of piezolaminated plate with different electric condition of the piezoelectric layer. Buckling loads are found out for simply supported piezoelectric laminated plates. Piezolaminated plates consist of cross ply symmetric and antisymmetric orientation of laminates with piezolayer attached at the top and bottom of the plate. Results presented for buckling analysis of plates are verified with other numerical solution available in the literature and further results for future references are provided.

Keywords Buckling Analysis, Piezolaminated Plate, Higher Order Shear Deformation Theory

1. Introduction

Over the last two decades plenty of work has been carried out on analysis of piezoelectric laminated structures including smart beams, columns and plates. The increased use of piezolaminated smart structures in structural application is stimulating development of different methods and solution techniques for the accurate analysis of piezolaminated structures. Some of these methods are Galerkin method, Finite element method, and Reddy's higher order shear deformation theory. Also the experimental investigation of smart piezolaminated structures has attracted some attention. The need of such smart structures with high stiffness and low weight in engineering applications has led to the gradual replacement of many isotropic materials/structures with light weight piezo-composites. The piezoelectric material possesses a coupled electromechanical property having a direct and converse piezoelectric effect. The availability of these piezoelectric ceramics in the form of thin sheet makes them well suited for use as distributed sensors and actuators to control structural response in shape, vibration and buckling.

Berlincourt et al.[1] and Mason[2] discussed the fundamentals of piezoelectricity in brief. Takagi[3] presented definition of smart materials and structures with notable arguments and detailed comments. The limitations of classical plate theory and first order shear deformation

theories forced the development of higher order theories to avoid the use of shear correction factors, to include correct cross sectional warping and to get the realistic variation of the transverse shear strains and stresses through the thickness of plate.

Tzou and Zhou[4] studied linear dynamics and distributed control of piezoelectric laminated continua. Donthireddy and Chandrashekhara[5] developed a mathematical model based on a layerwise theory for laminated composite beams with piezoelectric actuators to study its shape control. Soares et al.[6] analysed piezolaminated composite plates using refined finite element models based on higher order displacement fields and studied structural optimization. Artael and Becker[7] investigated numerically the effect of electro-mechanical coupling on the interlaminar stresses and the electric field strengths at free edges of piezolaminated plates. Oh and Lee[8] studied geometric nonlinear analysis of cylindrical piezolaminated shells based on the multifield layerwise theory using finite element method for the thermal and piezoelectric loading. Tzou and Gadre[9, 10] carried out theoretical analysis for vibration control of a multilayered thin shell coupled with piezoelectric actuators. Batra and Liang[11] analysed the steady state vibrations of a simply supported rectangular elastic laminated plate with embedded PZT layers. They used three dimensional linear theory of elasticity. Oh et al.[12] worked on postbuckling and vibration characteristics of piezolaminated composite plate subject to thermo-piezoelectric loads. Shen[13, 14] presented post

buckling of shear deformable laminated plates with piezoelectric actuators under complex loading condition including thermo-electro-mechanical loading. Wang[15]

* Corresponding author:

rajanw04@gmail.com (Rajan L. Wankhade)

Published online at <http://journal.sapub.org/cmaterials>

Copyright © 2013 Scientific & Academic Publishing. All Rights Reserved

investigated elastic buckling of column structures with a pair of piezoelectric layers surface bonded on both sides of the columns. The governing equation coupling the piezoelectric effect was derived based on the assumed distribution of the electric potential in the flexural direction of the piezoelectric layer and an eigenvalue problem was solved using the direct difference method. Liew et al[16] carried out stability of piezoelectric FGM rectangular plates subjected to non-uniformly distributed load, heat and voltage. For carrying out analysis element free Galerkin method was employed.

In the present work stability analysis of piezolaminated plates is carried out considering higher order shear deformation theory. Piezolaminated plate studied is subjected to combined action of electromechanical loading. Linear through-the-thickness electric potential distribution is assumed for each piezoelectric sub-layer. Temperature field is assumed to be uniform for the orthotropic layers of the laminate and for piezolayer. Finite element formulation considers an isoperimetric eight noded rectangular element. Parametric studies are conducted to demonstrate the influence of boundary condition, ply orientation and plate aspect ratio on stability of piezolaminated plate with different electric condition of the piezolayer. Numerical results are presented considering simply supported and clamped piezoelectric laminated plate.

2. Finite Element Formulation

Finite element formulation is based on higher order shear deformation theory which do not need shear correction factor as that of first order shear deformation theory. And hence for considering the effect of shear deformation displacement field of HOST is assumed as follows

$$\begin{aligned} u &= u_0 + z\theta_x + z^2u_0^* + z^3\theta_x^* \\ v &= v_0 + z\theta_y + z^2v_0^* + z^3\theta_y^* \\ w &= w_0 \end{aligned} \quad (1)$$

Where, u , v and w are the displacement of any point in the plate domain in x , y and z direction respectively. u_0 , v_0 and w_0 are the displacement of midpoint of normal. θ_x , θ_y are the rotations of normal at the middle plane in x and y direction about y and x axis respectively. u_0^* , v_0^* , w_0^* , θ_x^* and θ_y^* are higher order terms which accounts cubic variation of normal.

Figure 1. shows a piezolaminated composite plate provided with piezoelectric patches at top and bottom surface of the plate. Fiber can be oriented with reference to the horizontal axes and is modelled in finite element formulation.

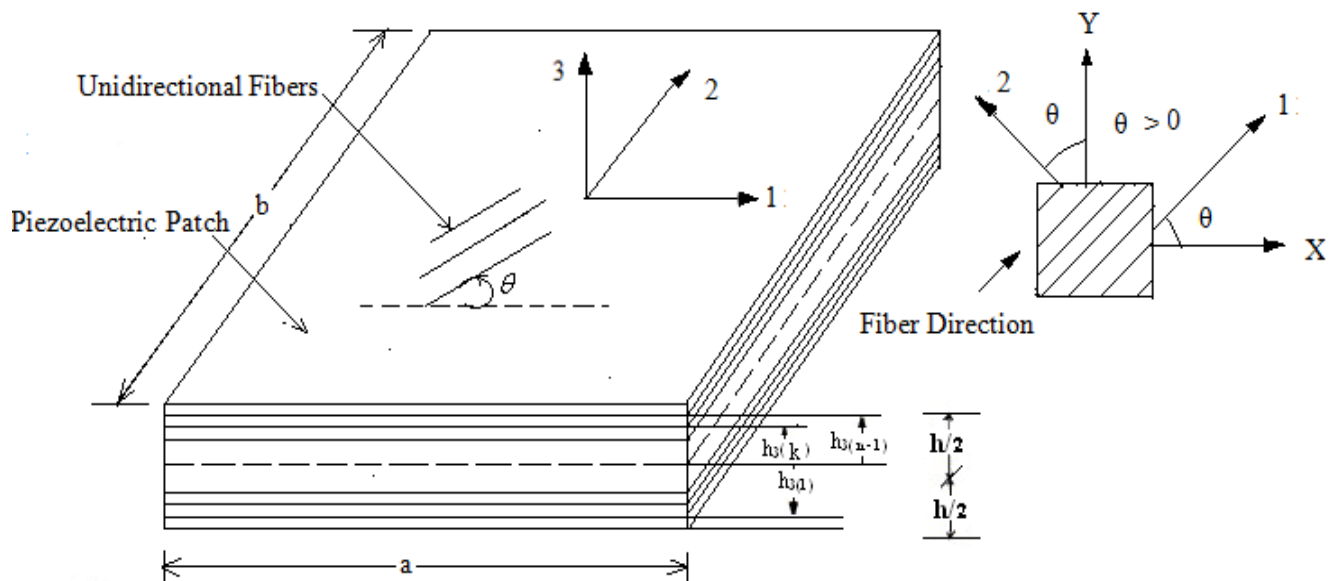


Figure 1. Piezolaminated composite plate provided with piezoelectric patches at top and bottom surface

Strain-Displacement Relations

The strains associated with the displacement model as per higher order shear deformation theory are given by

$$\begin{aligned}\varepsilon_x &= \varepsilon_{x0} + z\chi_x + z^2\varepsilon_{x0}^* + z^3\chi_x^* \\ \varepsilon_y &= \varepsilon_{y0} + z\chi_y + z^2\varepsilon_{y0}^* + z^3\chi_y^* \\ \varepsilon_z &= \varepsilon_{z0} + z\chi_z + z^2\varepsilon_{z0}^* + z^3\chi_z^* \\ \gamma_{xy} &= \varepsilon_{xy0} + z\chi_{xy} + z^2\varepsilon_{xy0}^* + z^3\chi_{xy}^* \\ \gamma_{xz} &= \varphi_x + z\chi_{xz} + z^2\varphi_x^* + z^3\chi_{xz}^* \\ \gamma_{yz} &= \varphi_y + z\chi_{yz} + z^2\varphi_y^* + z^3\chi_{yz}^*\end{aligned}\quad (2)$$

Where,

$$\begin{aligned}\begin{bmatrix} \varepsilon_{x0} & \varepsilon_{y0} & \varepsilon_{z0} & \varepsilon_{xy0} \end{bmatrix}^T &= \begin{bmatrix} \frac{\partial u_0}{\partial x} & \frac{\partial v_0}{\partial y} & \theta_x & \frac{\partial u_0}{\partial y} + \frac{\partial v_0}{\partial x} \end{bmatrix}^T \\ \begin{bmatrix} \chi_x & \chi_y & \chi_z & \chi_{xy} \end{bmatrix}^T &= \begin{bmatrix} \frac{\partial \theta_x}{\partial x} & \frac{\partial \theta_y}{\partial y} & 2w_0^* & \frac{\partial \theta_x}{\partial y} + \frac{\partial \theta_y}{\partial x} \end{bmatrix}^T \\ \begin{bmatrix} \varepsilon_{x0}^* & \varepsilon_{y0}^* & \varepsilon_{xy0}^* \end{bmatrix}^T &= \begin{bmatrix} \frac{\partial u_0^*}{\partial x} & \frac{\partial v_0^*}{\partial y} & \frac{\partial u_0^*}{\partial y} + \frac{\partial v_0^*}{\partial x} \end{bmatrix}^T \\ \begin{bmatrix} \chi_x^* & \chi_y^* & \chi_{xy}^* \end{bmatrix}^T &= \begin{bmatrix} \frac{\partial \theta_x^*}{\partial x} & \frac{\partial \theta_y^*}{\partial y} & \frac{\partial \theta_x^*}{\partial y} + \frac{\partial \theta_y^*}{\partial x} \end{bmatrix}^T \\ \begin{bmatrix} \phi_x^* & \phi_y^* \end{bmatrix}^T &= \begin{bmatrix} 3\theta_x^* \frac{\partial w_0^*}{\partial x} & 3\theta_y^* \frac{\partial w_0^*}{\partial y} \end{bmatrix}^T \\ \begin{bmatrix} \psi_x & \psi_y \end{bmatrix}^T &= \begin{bmatrix} 2u_0 + \frac{\partial \theta_z}{\partial x} & 2v_0 + \frac{\partial \theta_z}{\partial y} \end{bmatrix}^T\end{aligned}\quad (3)$$

Shell Element and Shape functions

8-node rectangular element is employed as shown in figure

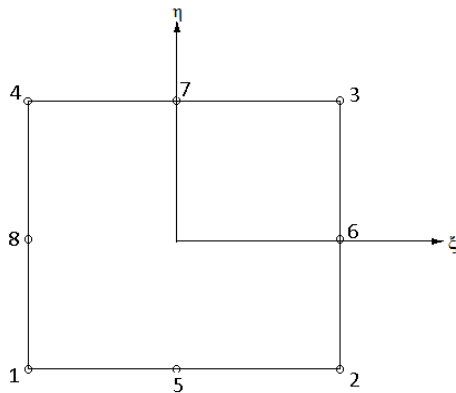


Figure 2. Eight-nodded rectangular element

Shape functions are given as,

For corner nodes:

$$N_i(\xi, \eta) = \frac{1}{4}(1 + \xi\xi_i)(1 + \eta\eta_i)(-1 + \xi\xi_i + \eta\eta_i),$$

for $i = 1, 2, 3, 4$

For middle edge node

$$\begin{aligned}N_5(\xi, \eta) &= \frac{1}{2}(1 - \xi^2)(1 - \eta) \\ N_7(\xi, \eta) &= \frac{1}{2}(1 - \xi^2)(1 + \eta) \\ N_6(\xi, \eta) &= \frac{1}{2}(1 + \xi)(1 - \eta^2) \\ N_8(\xi, \eta) &= \frac{1}{2}(1 - \xi)(1 - \eta^2)\end{aligned}\quad (4)$$

Displacement field

The displacement field associated with the eight noded element can be written as

$$\begin{aligned}u &= \sum_{i=1}^8 N_i u_i \\ v &= \sum_{i=1}^8 N_i v_i \\ w &= \sum_{i=1}^8 N_i w_i\end{aligned}\quad (5)$$

Strain within the Element

Strains associated with the displacement field can be written as follow,

a. Middle plane membrane strains

$$\underbrace{\varepsilon_p}_{3 \times 1} = \varepsilon_p^L + \varepsilon_p^N \quad (6)$$

in which ε_p^L and ε_p^N are linear and non-linear components of middle plane membrane strains and combining linear and non-linear terms membrane strains are given as,

$$\underbrace{\varepsilon_p}_{3 \times 1} = \left\{ \begin{array}{c} \frac{\partial u}{\partial x} \\ \frac{\partial v}{\partial y} \\ \frac{\partial u}{\partial y} + \frac{\partial v}{\partial x} \end{array} \right\} + \left\{ \begin{array}{c} \frac{1}{2} \left(\frac{\partial w}{\partial x} \right)^2 \\ \frac{1}{2} \left(\frac{\partial w}{\partial y} \right)^2 \\ \frac{\partial w}{\partial x} \cdot \frac{\partial w}{\partial y} \end{array} \right\} \quad (7)$$

Curvature strains/Bending strains

Curvature strains are linearly related to bending displacement as,

$$\varepsilon_b^L = \left\{ \begin{array}{c} \varepsilon_{xxb} \\ \varepsilon_{yyb} \\ \varepsilon_{xyb} \end{array} \right\}$$

$$= z \begin{Bmatrix} \frac{\partial \theta_x}{\partial x} \\ \frac{\partial \theta_y}{\partial y} \\ \frac{\partial \theta_x}{\partial y} + \frac{\partial \theta_y}{\partial x} \end{Bmatrix} = z.K \quad (8)$$

Shear strains, $\underline{\gamma}_{2 \times 1} = \begin{Bmatrix} \gamma_{xz} \\ \gamma_{yz} \end{Bmatrix}$

$$= \begin{Bmatrix} \theta_x + \frac{\partial w}{\partial x} \\ \theta_y + \frac{\partial w}{\partial y} \end{Bmatrix} \quad (9)$$

Thus

$$\begin{Bmatrix} \underline{\varepsilon} \\ \underline{\gamma} \end{Bmatrix}_{6 \times 1} = \begin{Bmatrix} \underline{\varepsilon}_p \\ \underline{\varepsilon}_b \end{Bmatrix}_{3 \times 1}$$

$$= \begin{Bmatrix} \underline{\varepsilon}_p^L \\ \underline{\varepsilon}_b^L \end{Bmatrix} + \begin{Bmatrix} \underline{\varepsilon}_p^N \\ 0 \end{Bmatrix} \quad (10)$$

Hence,

$$\underline{\varepsilon}_{6 \times 1} = \underline{\varepsilon}_{6 \times 1}^L + \underline{\varepsilon}_{6 \times 1}^N \quad (11)$$

and shear strains can separately be written as,

$$\underline{\gamma}_{2 \times 1} = \begin{Bmatrix} \gamma_{xz} \\ \gamma_{yz} \end{Bmatrix} \quad (12)$$

In which $\{\varepsilon_p\}$, $\{\varepsilon_b\}$ and $\{\gamma\}$ are membrane, bending and shear components of strains respectively. $\underline{\varepsilon}_{6 \times 1}$ is combined

strain vector of membrane and bending strains. $\underline{\gamma}_{2 \times 1}$ is a vector containing shear strains. Subscript 'p' stands for in-plane, 'b' for bending, 'L' for linear and subscript 'N' stands for non-linear.

Displacement-strain relation

Strains are related with displacements using strain displacement matrix as follows,

$$\underline{\varepsilon} = B \underline{\delta}_e \quad (13)$$

Electro-Mechanical Coupling

For piezolaminated plates two constitutive relationships exist including the effect of mechanical and electrical loading as given by eq. 14. Variation of temperature effect is neglected in formulation.

$$\{D\} = [e]\{\varepsilon\} + [g]\{E^p\}$$

$$\{\sigma\} = [C]\{\varepsilon\} - [e]^t \{E^p\} \quad (14)$$

And hence,

$$\begin{Bmatrix} \sigma'_x \\ \sigma'_y \\ \sigma'_z \\ \sigma'_{xy} \\ \sigma'_{xz} \\ \sigma'_{yz} \end{Bmatrix} = \begin{bmatrix} Q_{11}' & Q_{12}' & Q_{13}' & Q_{14}' & 0 & 0 \\ Q_{21}' & Q_{22}' & Q_{23}' & Q_{24}' & 0 & 0 \\ Q_{31}' & Q_{32}' & Q_{33}' & Q_{34}' & 0 & 0 \\ Q_{14}' & Q_{24}' & Q_{34}' & Q_{44}' & 0 & 0 \\ 0 & 0 & 0 & 0 & Q_{55}' & Q_{56}' \\ 0 & 0 & 0 & 0 & Q_{65}' & Q_{66}' \end{bmatrix} \begin{Bmatrix} \varepsilon'_x \\ \varepsilon'_y \\ \varepsilon'_z \\ \varepsilon'_{xy} \\ \varepsilon'_{xz} \\ \varepsilon'_{yz} \end{Bmatrix} \quad (15)$$

$$- \begin{bmatrix} 0 & 0 & e_{z1} \\ 0 & 0 & e_{z2} \\ 0 & 0 & e_{z3} \\ 0 & e_{y5} & 0 \\ e_{x6} & 0 & 0 \end{bmatrix} \begin{Bmatrix} E^p_x \\ E^p_y \\ E^p_z \end{Bmatrix}$$

Where, $\{D\}$ is electric displacement vector, $[e]$ is dielectric permittivity matrix, ε is the strain vector, $\{g\}$ is the dielectric matrix. $\{E\}$ is the electric field vector, $\{\sigma\}$ is the stress vector and $[C]$ is the elastic matrix for constant electric field.

Electrical Potential Function

ϕ'_a and ϕ'_s are the electric displacement at any point in the actuator and the sensor layers, respectively, the electrical potential functions in terms of the nodal potential vector are given by

$$\begin{aligned} \phi'_a &= [N_{pa}] \{\phi_a^e\} \\ \phi'_s &= [N_{ps}] \{\phi_s^e\} \end{aligned} \quad (16)$$

Where, $[N_{pa}]$ and $[N_{ps}]$ are the shape function matrices for the actuator and sensor layers, respectively. $\{\phi_a^e\}$ and $\{\phi_s^e\}$ are the nodal electric potential vector for the actuator and sensor layers respectively and can be given as follow.

$$\begin{aligned} \{\phi_a^e\} &= \{\phi_{a1} \ \phi_{a2} \ \phi_{a3} \dots \phi_{an}\}^T \\ \{\phi_s^e\} &= \{\phi_{s1} \ \phi_{s2} \ \phi_{s3} \dots \phi_{sn}\}^T \end{aligned} \quad (17)$$

Stiffness Matrix Equations

Element stiffness matrix can be written as,

$$[K^e] \{\delta^e\} + [K_\sigma^e] \{\delta^e\} = [F_1^e] + [F_{ac}^e] \quad (18)$$

In which

$$[K^e] = [K_d^e] + [K_{aa}^e]^{-1} [K_{aa}^e] [K_{ad}^e] + [K_{ds}^e] [K_{ss}^e]^{-1} [K_{sd}^e] \quad (19)$$

$$[F_{ac}^e] = [K_{da}^e] [K_{aa}^e]^{-1} \{Q_a^e\} \quad (20)$$

Where,

$$[K_d^e] = \int_V [B]^T [C] [B] dV,$$

$$[K_{da}^e] = [K_{ad}^e]^T = \int_{V_a} [B]^T [e] [B_a] dV,$$

$$\begin{aligned}
 [K_{aa}^e] &= \int_{V_a} [B_a]^T [g][B_a] dV, \\
 [K_{ds}^e] &= [K_{sd}^e]^T = \int_{V_s} [B]^T [e][B_s] dV \\
 \text{and } [K_{ss}^e] &= \int_{V_s} [B_s]^T [g][B_s] dV \quad (21)
 \end{aligned}$$

Thus the element equation in the global stiffness matrix can be written as

$$[K]\{\delta\} + [K_\sigma]\{\delta\} = [F_1] + [F_{ac}] \quad (22)$$

Equilibrium and incremental Equations

Virtual displacement principle is employed to obtain equilibrium equation. Equilibrium between internal and external forces has to be satisfied. If Ψ represents the vector of the sum of the internal and external forces.

$$\{\Psi\} = \{R\} - \{P\} \quad (23)$$

Where, $\{R\}$ represents the external forces due to imposed load and $\{P\}$ is a vector of internal resisting forces. The equilibrium state is achieved when $\{\Psi\} = 0$.

$$\begin{aligned}
 \{\Psi\} &= \{R\} + \frac{1}{2} \int_V \{\varepsilon\}^T \{\sigma\} dV \\
 &- \frac{1}{2} \int_{V_a} [E_a^p]^T \{D_a\} dV \\
 &- \frac{1}{2} \int_{V_s} [E_s^p]^T \{D_s\} dV + \int_V \{\varepsilon^N\}^T \{\sigma_0\} dV
 \end{aligned} \quad (24)$$

Where V , V_a and V_s are the area of the entire structure, sensor layer and actuator layer respectively. Considering the work done by external forces due to the applied surface

traction and applied electric charge on actuator the equation for external work done can be written as

$$\{R\} = \int_A \left\{ \begin{matrix} u \\ - \end{matrix} \right\}^T \left\{ \begin{matrix} \sigma \\ - \end{matrix} \right\} (x, y) dA + \int_A \phi_a' \bar{q}_a^e(x, y) dA \quad (25)$$

Stability equation

The geometric stiffness matrix is associated with the x and y coordinates. The characteristic equation of stability is written as,

$$([K] + \lambda[K_\sigma]) \{\delta\} = F \quad (26)$$

$$([K] + \lambda[K_\sigma]) (\{\delta\} + \{d\delta\}) = \{F\} \quad (27)$$

Where, the lowest magnitude of eigen value gives critical buckling load and the vector $\{d\delta\}$ represents the buckled mode shape. And the eigen value problem is solved to get buckling loads.

$$([K] + \lambda[K_\sigma]) \{d\delta\} = 0 \quad (28)$$

3. Results and Discussions

Buckling analysis of piezolaminated plates have been carried out for different ply orientation considering symmetric and antisymmetric cross-ply lamination schemes. Buckling of smart piezolaminated plate is examined subjected to uniform axial compressive force at the edges. Furthermore for piezolaminated plate, critical mechanical buckling loads are obtained for different thickness to span ratios of piezolaminated plates and for closed and open loop electric condition.

3.1. Buckling of Simply Supported Square Multilayered Plate (0°/90°...)_n

Table 1. Non-dimensional critical buckling load ($\bar{N} = \sigma_{cr} b^2 / E_2 h^2$) for simply supported multilayered cross ply laminated plate

a/h	theory	Layer	Degree of Orthotropy (E_1 / E_2)				
			3	10	20	30	40
5	present	3	4.5479	7.1726	9.4143	10.8521	11.8872
	Owen and Li [17]		4.5597	7.1758	9.4178	10.8573	11.8867
10	present		5.4031	9.9543	15.3227	19.6863	23.3341
	Owen and Li [17]		5.4026	9.9590	15.3201	19.6872	23.3330
20	present		5.6578	11.0735	18.3872	25.2481	31.6928
	Owen and Li [17]		5.6679	11.0727	18.3879	25.2476	31.6949
50	present		5.7546	11.4457	19.5111	27.4985	35.3947
	Owen and Li [17]		5.7521	11.4414	19.5135	27.4983	35.3957
100	present		5.7641	11.5081	19.7069	27.8731	36.0231
	Owen and Li [17]		5.7680	11.5048	19.7000	27.8727	36.0220
5	present	5	4.6011	7.5455	10.2731	12.1089	12.8271
	Owen and Li [17]		4.6078	7.5445	10.2727	12.0834	12.8344
10	present		5.4221	10.1611	15.9969	20.9499	25.1145
	Owen and Li [17]		5.4208	10.1609	15.9976	20.9518	25.2150
20	present		5.6734	11.1364	18.6426	25.7910	32.5842
	Owen and Li [17]		5.6730	11.1370	18.6413	25.7923	32.6137
50	present		5.7527	11.4585	19.5615	27.6044	35.4832
	Owen and Li [17]		5.7531	11.4531	19.5605	27.6037	35.5819
100	present		5.7675	11.5018	19.7136	27.9037	36.0621
	Owen and Li [17]		5.7683	11.5086	19.7140	27.9028	36.0740

Effect of orthotropy is studied for simply supported square multilayered plate subjected to a uniform uniaxial compressive force at the edges. Laminated plate is having cross ply orientation of layers. Critical buckling loads are tabulated in Table 1 for effect of orthotropy of individual layers, the ratio of span to thickness (a/h) and the number of layers of simply supported square multilayered composite plates. Material property adopted is as follow.

$$\frac{E_1}{E_2} = 3 \text{ to } 40, \frac{E_3}{E_2} = 1, \frac{G_{12}}{E_2} = \frac{G_{13}}{E_2} = 0.6,$$

$$\frac{G_{23}}{E_2} = 0.5 \text{ and } \mu_{12} = \mu_{13} = \mu_{23} = 0.25$$

Results are found in good agreement with that of refined finite element solution given by Owen and Li [17].

3.2. Buckling of Simply Supported Square Piezoelectric Laminated Plate (p/0⁰/90⁰/90⁰/0⁰/p)

The piezoelectric laminate with piezolayer attached at the top and bottom of the plate is subjected to a uniaxial uniform edge compressive force N_x . Hence a square piezoelectric laminated plate of thickness of 0.01 m and side length ‘a’ is having simply supported boundary on all four edges. The laminate consists of a (p/0⁰/90⁰/90⁰/0⁰/p) Graphite-Epoxy sublaminate provided with two PZT-5A attached on outer surface of the plate. Each piezoelectric layer has thickness of 0.1h, whereas each elastic layer has a thickness of 0.2h. Elastic and piezoelectric material properties are as shown in table 2.

Table 2. Elastic and piezoelectric properties for Graphite-Epoxy and PZT-5

Properties	Elastic Properties		Piezoelectric Properties		
	Grphite-Epoxy	PZT -5A	Properties	Grphit-Epoxy	PZT-5A
E_{11} (Gpa)	181	61.0	d_{31} (10^{-12} m/V)	0	-171
E_{22} (Gpa)	10.3	61.0	d_{32} (10^{-12} m/V)	0	-171
E_{33} (Gpa)	10.3	53.2	d_{33} (10^{-12} m/V)	0	374
G_{12} (GPa)	7.17	22.6	d_{15} (10^{-12} m/V)	0	584
G_{23} (GPa)	2.87	21.1	d_{24} (10^{-12} m/V)	0	584
G_{32} (GPa)	7.17	21.1	g_{11} (10^{-8} F/m)	0.0031	1.53
ν_{12}	0.28	0.35	g_{22} (10^{-8} F/m)	0.0027	1.53
ν_{23}	0.28	0.38	g_{33} (10^{-8} F/m)	0.0027	1.5
ν_{32}	0.33	0.38			

The effect of span to thickness ratio on critical uniaxial buckling load ($N_x a^2/E_2 h^3$) of simply supported square laminated plate with different electric condition is shown in figure 3.

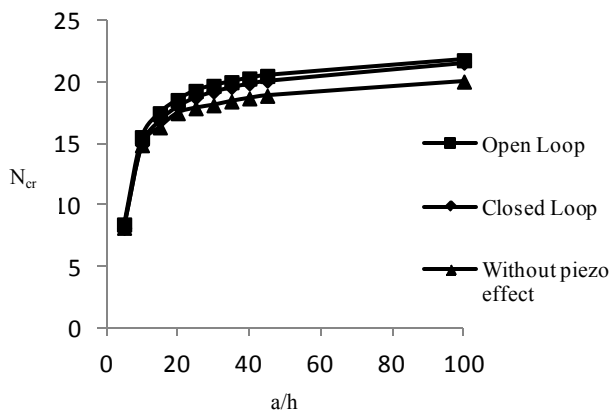


Figure 3. Effect of span to thickness ratio on normalized critical buckling load of simply supported symmetric cross ply piezolaminated plate (p/0⁰/90⁰/90⁰/0⁰/p)

From figure 3 it can be observed that critical buckling load increases for piezoelectric effect. Also piezoelectricity has little effect on the buckling load of the laminates with closed-circuits than that of open loop. There is an increase of 7.9 % in critical buckling load for piezolaminated plate than that of without piezoeffect. Hence critical buckling load can be considerably increases if plate is subjected to piezoeffect. For lesser vaues of a/h ratio % variation in critical buckling load is found to be 3.3 % for open loop electric condition than that of closed loop.

3.3. Buckling of Simply Supported Square Piezoelectric Laminated Plate (p/0⁰/90⁰/0⁰/90⁰/p)

Simply supported square piezolaminates with piezolayer attached at the top and bottom of the plate is subjected to a uniaxial uniform edge compressive force N_x . Piezoelectric laminated plate is having a thickness of 0.01 m and side length ‘a’. The laminate consists of antisymmetric ply orientation of Graphite-Epoxy sublaminate provided with two PZT-5A attached on outer surfaces of the plate. Material properties of Graphite-Epoxy and PZT-5A are same as

previous example. Each piezoelectric layer has thickness of $0.1h$, whereas each elastic layer has a thickness of $0.2h$. Figure 4 shows effect of span to thickness ratio on critical mechanical buckling load ($N_x a^2/E_2 h^3$) of piezolaminated plate with different electric conditions.

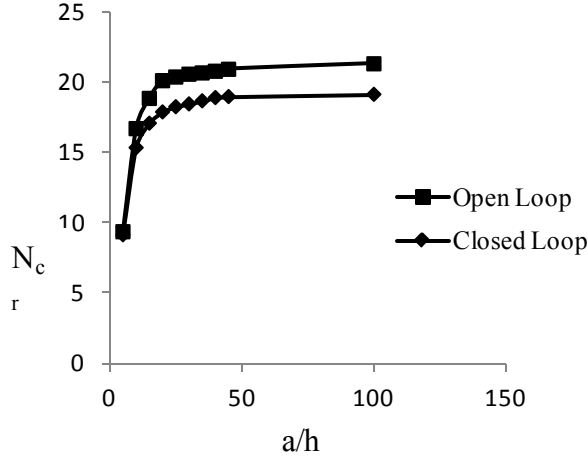


Figure 4. Effect of span to thickness ratio on normalized critical buckling load of simply supported antisymmetric cross ply piezolaminated plate ($p_0^0/90^0/0^0/90^0/p$)

Significant increase in critical buckling load is observed for open loop electric condition than that of closed loop. Thus piezoelectricity has little effect on the buckling load of the laminates with closed-circuits in this case. The increase in critical buckling load is found to be 8.09 %, 11.05 % and 10.19 % for open loop circuit than that of closed loop for $a/h = 10, 20$ and 100 respectively.

4. Conclusions

A finite isoparametric element for the mechanical displacement field is combined with an electric potential field to consider piezoelectric effect. Parametric study is conducted to demonstrate the influence of boundary condition, ply orientation and plate aspect ratio on stability of piezolaminated plate with different electric condition of the piezolayer. For symmetric cross ply piezolaminated plate % increase in critical buckling load is found to be 7.9% than that of without piezoeffect. Thus considering piezoeffect buckling load can be considerably increased.

Appendix: Stiffness Coefficients of the Laminated Plate According to The Higher Order Shear Deformation Theory

The stiffness coefficients according to the HOST are as follows

$$Q_{11} = C_{11} \cos^4 \theta + 2(C_{12} + 2C_{33}) \sin^2 \theta \cos^2 \theta + C_{22} \sin^4 \theta$$

$$Q_{12} = C_{12} (\cos^4 \theta + \sin^4 \theta) + (C_{11} + C_{22} - 4C_{33}) \sin^2 \theta \cos^2 \theta$$

$$Q_{13} = (C_{11} - C_{12} - 2C_{33}) \sin \theta \cos^3 \theta + (C_{12} - C_{22} + 2C_{33}) \cos \theta \sin^3 \theta$$

$$Q_{22} = C_{11} \sin^4 \theta + 2(C_{12} + 2C_{33}) \sin^2 \theta \cos^2 \theta + C_{22} \cos^4 \theta$$

$$Q_{23} = (C_{11} - C_{12} - 2C_{33}) \sin^3 \theta \cos \theta + (C_{12} - C_{22} + 2C_{33}) \cos^3 \theta \sin \theta$$

$$Q_{33} = (C_{11} - 2C_{12} + C_{22} - 2C_{33}) \sin^2 \theta \cos^2 \theta + C_{33} (\cos^4 \theta + \sin^4 \theta)$$

$$Q_{44} = C_{44} \cos^2 \theta + C_{55} \sin^2 \theta$$

$$Q_{45} = (C_{44} - C_{55}) \sin \theta \cos \theta$$

$$Q_{55} = C_{44} \sin^2 \theta + C_{55} \cos^2 \theta$$

$$Q_{ij} = Q_{ji} \text{ for } i, j = 1, 2, \dots, 5$$

Where,

$$C_{xx} = \frac{E_x (1 - \nu_{yz} \nu_{zy})}{\nu^*};$$

$$C_{yy} = \frac{E_y (1 - \nu_{xz} \nu_{zx})}{\nu^*};$$

$$C_{zz} = \frac{E_z (1 - \nu_{xy} \nu_{yx})}{\nu^*};$$

$$C_{xy} = \frac{E_x (\nu_{yx} + \nu_{zx} \nu_{yz})}{\nu^*};$$

$$C_{xz} = \frac{E_x (\nu_{zx} + \nu_{yx} \nu_{zy})}{\nu^*};$$

$$C_{yz} = \frac{E_y (\nu_{zy} + \nu_{xy} \nu_{zx})}{\nu^*} \quad G_{xy} = \frac{C_{xy}}{k};$$

$$G_{zx} = \frac{C_{zx}}{k}; \quad G_{yz} = \frac{C_{yz}}{k};$$

And

$$\nu^* = 1 - (\nu_{xy} \nu_{yx} + \nu_{yz} \nu_{zy} + \nu_{zx} \nu_{xz} + 2\nu_{yx} \nu_{zy} \nu_{xz})$$

REFERENCES

- [1] D. A. Berlincourt, D. R. Curran and H. Jaffe, "Piezoelectric and piezomagnetic materials and their functions in transducers", In: Mason W. P. (Ed.), Physical Acoustics, 1, Academic New York, pp. 169-270, 1964.
- [2] W. P. Mason, "Piezoelectricity, its history and applications", The Journal of Acoustical Society of America, vol.70, pp. 1561-1566, 1981.
- [3] T. Takagi, "A concept of intelligent materials", Journal of Intelligent Materials, Systems and Structures, vol.1, pp. 149-56, 1990.
- [4] Tzou, H. S., Zhou, Y. H. (1995). "Dynamics and control of non-linear circular plates with piezoelectric actuators", Journal of Sound and Vibration, 188 (2), pp. 189-207.

- [5] P. Dhonthireddy, K. Chandrashekhara, "Modeling and shape control of composite beams with embedded piezoelectric actuators", *Composite Structures*, vol.35, pp. 237-244, 1996.
- [6] C. M.M. Soares, C. A. M. Soares, V. M. F. Correia, "Optimal design of piezolaminated structures", *Composite Structures*, vol. 47, pp. 625-634, 1999.
- [7] J. Artel, W. Becker, "Coupled and uncoupled analyses of piezoelectric free-edge effect in laminated plates", *Composite Structures*, vol. 69, pp. 329-335, 2005.
- [8] I. K. Oha, I. Lee, "Supersonic flutter suppression of piezolaminated cylindrical panels based on multifield layerwise theory", *Journal of Sound and Vibration*, vol. 291, pp. 1186-1201, 2006.
- [9] H. S. Tzou, M. Gadre, M. "Active vibration isolation and excitation by piezoelectric slab with constant feedback gains", *Journal of Sound and Vibration*, vol. 136 (3), pp. 477-490, 1989
- [10] H. S. Tzou, M. Gadre, "Theoretical analysis of a multilayered thin shell coupled with piezoelectric shell actuator for distributed vibration controls", *Journal of Sound and Vibration*, vol. 132 (3), pp 433-450, 1990.
- [11] R. C. Batra, X. Q. Liang, "The vibration of a rectangular laminated elastic plate with embedded piezoelectric sensors and actuators", *Computers and Structures*, vol. 63 (2), pp. 203-216, 1997.
- [12] I. K. Oh, J. H. Han, I. Lee, "Postbuckling and vibration characteristics of piezolaminated composite plate subject to thermo-piezoelectric loads", *Journal of Sound and Vibration*, vol.233 (1), pp. 19-40, 2000.
- [13] H. S. Shen, "Postbuckling of shear deformable laminated plates with piezoelectric actuators under complex loading condition", *International Journal of Solids and structures*, vol.38, pp. 7703-7721, 2001.
- [14] H. S. Shen, "Thermal postbuckling of shear deformable laminated plates with piezoelectric actuators", *Composite Science and Technology*, vol.61, pp. 1931-1943, 2001.
- [15] Q. Wang, "On buckling of column structures with a pair of piezoelectric layers", *Engineering structures*, vol. 24, pp. 199-205, 2002.
- [16] K. M. Liew, J. Yang, S. Kitipornchai, "postbuckling of piezoelectric FGM plates subject to thermo - electro - mechanical loading", *International Journal of Solids and Structures*, vol. 40, pp. 3869-3892, 2003.
- [17] D. R. J. Owen and Z. H. Li, "A refined analysis of laminated plates by finite element displacement methods-II. Vibration and stability", *Computers and Structures*, vol.26 (6), pp. 915-923, 1987.